Influence of Perovskite Termination on Oxide Heteroepitaxy

D. A. Schmidt*
Dept. of Physics & Center for Nanotechnology (CNT), Univ. of Washington (UW), Seattle, WA 98195-1560

Taisuke Ohta†
Dept. of Mat. Sci. and Engin. & CNT, UW, Seattle, WA 98195-2120

Q. Yu‡
Dept. of Physics, UW, Seattle, WA 98195-1560

Marjorie A. Olmstead
Dept. of Physics & CNT, UW, Seattle, WA 98195-1560

(Dated: April 14, 2006)

We report a combined high temperature scanning tunneling microscopy, ion scattering and photoelectron spectroscopy study of bare lanthanum aluminate ($LaAlO_3$, LAO) and of the initial stages of anatase TiO_2 growth on LAO(001). LAO(001) exhibits mixed La-O and Al-O_2 surface terminations at 400°C. Heteroepitaxial TiO_2, grown by evaporating Ti metal in O_2, nucleates near step edges, growing out to cover both upper and lower terraces uniformly, regardless of termination, indicating that the substrate cations and perovskite surface polarity play little direct role controlling morphology of this single-metal oxide heteroepitaxy. TiO_2 films 1.5 nm thick exhibit a surface reconstruction similar to the bulk anatase (1×4).

PACS numbers: 68.47.-b, 68.55.-a, 68.37.Ef
Keywords: Lanthanum Aluminate, $LaAlO_3$, antase, TiO_2, oxide heteroepitaxy, scanning tunneling microscopy (STM)

I. INTRODUCTION

The alternating layer structure of $LaAlO_3(001)$, a commonly used substrate for growth of high T_c superconductors[1–4] and other perovskite-based materials,[5] raises interesting questions about the role of substrate cations and polarity in oxide heteroepitaxy. Depending on temperature and surface preparation, $LaAlO_3(001)$ surfaces may exhibit single-height (d = 1.89Å) steps separating terraces of alternating La-O and Al-O_2 termination, double-height ($2d$) steps between terraces of the same termination, or combinations thereof. The two terminations differ in their nominal charge: $La^{3+}O^{2-} = (\text{La-O})^+$ and $Al^{3+}(O^{2-})_2 = (\text{Al-O}_2)^-$. In growth of $SrTiO_3$ (STO) on $LaAlO_3$ (LAO)[5] and vice versa[6], the interface is believed to be either $(\text{Ti}-\text{O}_2)^0/(\text{La-O})^+$ or $(\text{Sr}-\text{O})^0/(\text{Al-O}_2)^-$, which would result in an excess 0.5 electron or hole, respectively, per interface unit cell. Mixed valence $Ti^{3+/4+}$ at a $(\text{Ti}-\text{O}_2)^0/(\text{La-O})^+$ interface accommodates this charge mismatch, leading to a stable interface with trapped electrons;[6] $(\text{Sr}-\text{O})^0/(\text{Al-O}_2)^-$ on the other hand, is insulating with numerous defects.[5,6]

Anatase TiO_2 is lattice matched to LAO (3.79 Å *vs.* 3.78 Å at room temperature); the neutral TiO_2 layer is buckled (unlike STO), and alternate layers change orientation rather than cation or polarity. Different interface structures and charges might be expected when TiO_2 is deposited on La-O or Al-O_2 terminated LAO. The spacing between low energy sites for positive and negative ions is $\sqrt{2}$ larger on the Al-O_2 termination than on La-O. Also, while the excess charge for the La-O termination may be absorbed by mixed valence $Ti^{3+/4+}$, similar to STO/LAO, the most likely candidates for balancing the excess charge of Al-O_2 termination are oxygen vacancies and exchange of Ti^{4+} with substrate Al^{3+}. Growth on Al-O_2 terminated regions might thus involve non-wetting, interdiffused, or oxygen deficient interfaces, perhaps accompanied by defect formation. Technological interest in growth of laminar, $\gtrsim$ 10 nm thick anatase films on LAO[7–11] for spintronic applications raises the question of whether the interface properties may be optimized by controlling the LAO surface termination.

Previous studies[5,12–15] have indicated that LAO(001) is terminated with Al-O_2 at room temperature, switching to La-O above ∼250°C; more recent studies[16] report both terminations at room temperature, but only La-O at temperatures above 727°C. In this paper, we report growth of the single-metal oxide TiO_2 on LAO surfaces prepared with roughly equal populations of La-O and Al-O_2 interspersed on the scale of several nanometers. Investigations with ion scattering spectroscopy (ISS), xray photoemission spectroscopy (XPS) and scanning tunneling microscopy (STM) surprisingly show no significant differences in TiO_2 nucleation and growth on the two terminations. Rather, TiO_2 nucleates at step edges and grows outward from single-height steps on both the upper and lower terraces, covering both La-O and Al-O_2 terraces uniformly before extensive nucleation of a second layer. When the film is 1.5 nm thick, it shows a

multi-domain (1×4) TiO_2 surface reconstruction similar to that[17–20] of crystalline anatase.

II. EXPERIMENTS

Commercially prepared (Princeton Scientific Corp.) LAO substrates were epi-polished on one side. Substrates were sonicated in methanol before vacuum-coating the non-polished side with a thin metal film (30 nm Ti followed by 90 nm Pt). The LAO was wiped clean with methanol prior to introduction in the ultrahigh vacuum (UHV) system (base pressure $<1\times10^{-10}$ torr). Substrates were were then annealed at 670°C, as measured with an optical pyrometer, in a partial pressure of molecular oxygen ($P_{O_2} = 5\times10^{-5}$ torr, purity >99.99%) for 25 minutes. Samples were resistively heated via the metal coating and/or a Si wafer in parallel with the sample. XPS showed the prepared LAO substrates to be free of carbon and other residual contaminants within an experimental resolution of 0.05 ML.

Thin ($\lesssim$ 1.5 nm) anatase TiO_2 films were deposited by molecular beam epitaxy (MBE). Pure (>99.99%) Ti metal was evaporated from an electron-beam evaporator in a background of O_2 at $P_{O_2} = 5\times10^{-5}$ torr at a substrate temperature $T_{sub} = 570$°C. A growth rate of 1 Å/min was measured by a water-cooled quartz crystal monitor. After growth, T_{sub} was lowered to 300°C in the presence of molecular oxygen to suppress oxygen vacancy formation. The oxygen was then evacuated while the sample was cooled to room temperature. The samples were then transferred under UHV to separate analysis (ISS, LEED, and XPS) and STM chambers. Film thickness estimates using XPS intensities from laminar films were consistent with those estimated from the quartz crystal monitor.

Core-level photoemission (XPS) was excited with a Mg K_α X-ray source. Ion scattering spectroscopy (ISS) was used to determine the surface elemental composition. The 500-1000 eV He^+ ions utilized yield sensitivity to only the exposed surface layer. To alleviate surface charging, as well as to probe the double-metal surface termination under growth-like conditions, elevated substrate temperatures of $T_{sub} = 400$°C were utilized for STM and ISS on the insulating bare LAO and submonolayer TiO_2 samples. For Fig. 2(c), a temperature of $T_{sub} = 60$°C (measured by thermocouple) was required for this small-scale imaging of a 4-5 molecular layer thick film, while large-scale STM [Fig. 1(c)] was obtained at room temperature. All STM bias voltages are measured with respect to a grounded sample.

III. RESULTS

A. Surface Morphology of Annealed LAO

The large-scale surface morphology of oxygen-anealed LAO(001) before deposition of TiO_2 is shown in Fig. 1(a). The bare, oxygen-annealed LAO(001) surface, imaged with HT-STM at 400°C, consists of long, ∼150 nm wide regions (labelled I and II in Fig. 1(a)) that have average heights differing by ∼0.4 nm, or one LAO unit cell. This implies that the base level on each terrace consists of the same termination (La-O or Al-O_2). Room temperature, non-contact atomic force microscopy (nc-AFM) of similarly prepared samples (not shown) reveals just this global step/terrace structure, with a mottled appearance on the terraces. The HT-STM results in Fig. 1(a) clearly show the terraces are neither atomically flat nor consisting of a single metal-oxide termination; rather, snakelike islands ∼10-20 nm in width and up to ∼40 nm in length are interspersed across the terraces. The result is a terrace consisting of a single, base surface termination with islands of possibly differing surface termination, depending on their height: "single-height" steps of height d = 1.89Å, or half the LAO unit cell, should alternate surface terminations, while "double-height" steps of height $2d$ separate terraces with the same La-O or Al-O_2 termination (see Fig. 4). Fig. 2(a) shows a high-resolution image of the border between regions I and II seen in Fig. 1(a), with solid white lines highlighting some steps of height $2d$ and dotted lines highlighting some single-height steps. The cross-section along the line A-A′ [Fig. 2(d)] shows numerous islands of height d and occasionally $2d$ scattered throughout, implying the surface has both La-O and Al-O_2 sublattices exposed. Surface termination by both cations was confirmed by ISS measurements of the surface elemental composition, also at 400°C, which indicated the presence of O, La, and Al at the surface (and no other atomic species).

B. Nucleation and Growth of Anatase TiO_2 on LAO(001)

Deposition of ∼0.5 molecular layers of TiO_2 on LAO(001) at 570°C does not significantly alter the large-scale surface morphology of the bare LAO (compare Figs. 1(a,b)): both show long terrace regions of average height difference $2d$, with smaller scale islands primarily of height d dispersed throughout. At smaller length scales [Fig. 2(b)], the nucleation of this sub-monolayer TiO_2 film may be seen. TiO_2 growth is seen both on the base of the terrace and on the islands (dotted white lines in Fig. 2(b) highlight some single step height edges). Darker regions near the centers of both island and terrace regions likely correspond to uncovered LAO, indicating the TiO_2 nucleates at steps and grows out to cover either terrace or island (solid white lines in Fig. 2(b)). For example, Fig. 2(e), which depicts the cross section

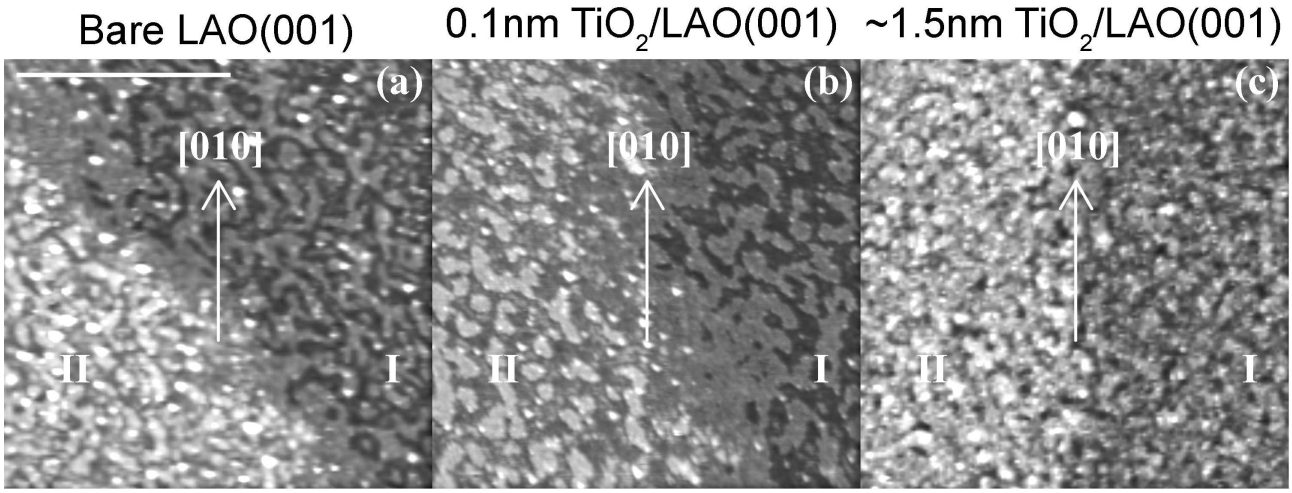

FIG. 1: **Large scale surface morphology of LAO(001) before and after deposition of TiO_2.** 200×200 nm^2 STM images of (a) bare LAO(001) annealed in 5×10^{-5} O_2 at 670°C, (b) ∼1 Å (∼0.5 ML) TiO_2 deposited at 570°C on post-annealed LAO(001), and (c) ∼15 Å TiO_2 deposited at 570°C on post-annealed LAO(001). Regions marked I and II in (a-c) have average heights differing by ∼0.4 nm, consistent with the 3.7 Å LAO unit cell height. Scale bare in (a) is 100 nm. Image conditions: (a,b) T_{sub} = 400°C, 4.5V, 0.08 nA; (c) T_{sub} = room temperature, 2.1V, 0.198 nA.

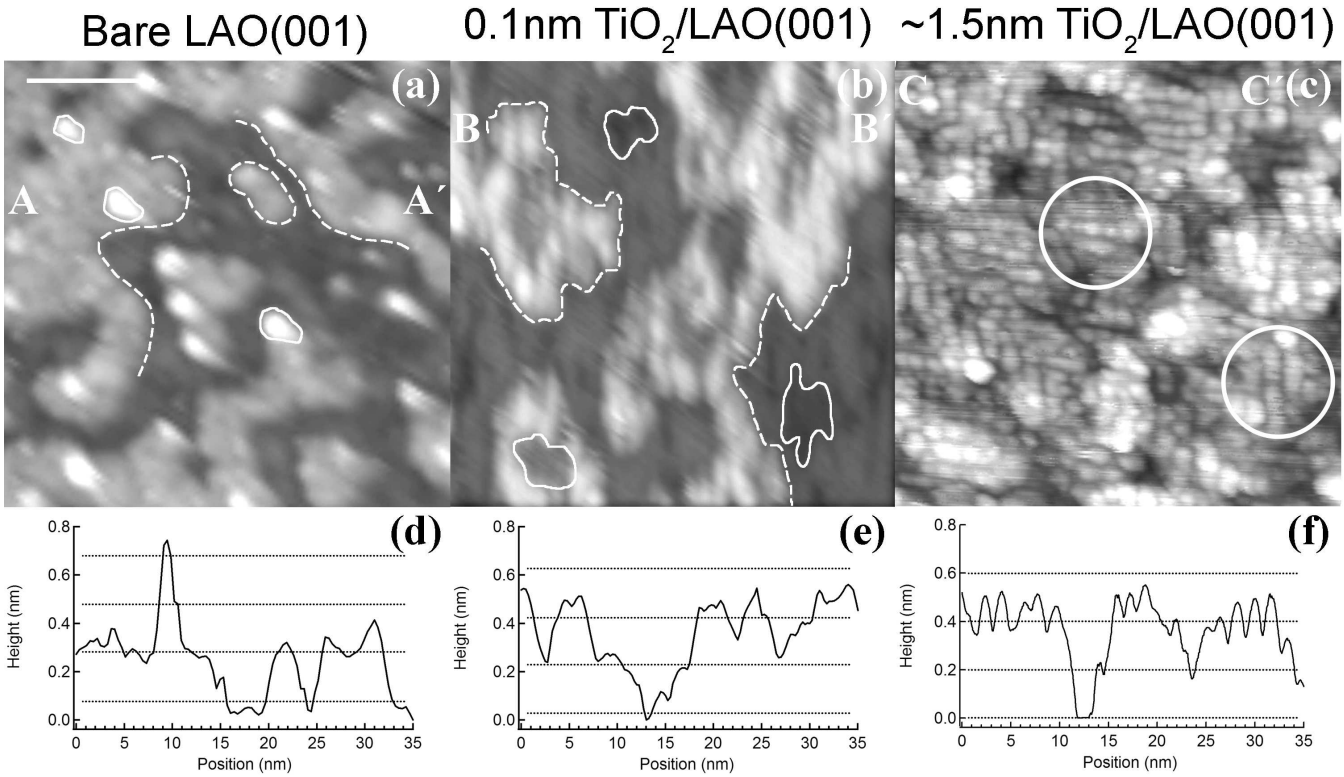

FIG. 2: **High resolution surface morphology of LAO(001) before after deposition of 1.5 nm TiO_2.** 35×35 nm^2 STM images of (a) bare LAO(001) annealed in 5×10^{-5} O_2 at 670°C, (b) ∼1 Å (∼0.5 ML) TiO_2 deposited at 570°C on post-annealed LAO(001), and (c) ∼15 Å TiO_2 deposited at 570°C on post-annealed LAO(001). (d-f) height *vs.* position along line connecting capital letters in (a-c). Horizontal dotted lines in (d-f) are single-step heights in LAO(001). Dashed white lines in (a) and (b) highlight some single-height (0.2 nm) steps. Solid white lines in (a) highlight some double-height (0.4 nm) steps, while in (b) highlight regions of no TiO_2 coverage. The circles in (c) indicate two domains of the 1×4 TiO_2 surface reconstruction, rotated by 90°. Scale bar in (a) is 10 nm. Images (a-c) have same orientation as those in Figs. 1(a-c). Image conditions: (a,b) T_{sub} = 400°C, 4.5V, 0.08 nA; (c) T_{sub} = 60°C, 4V, 0.16 nA.

along the line connecting points B and B′, shows growth across the terrace except areas which tend to be far from

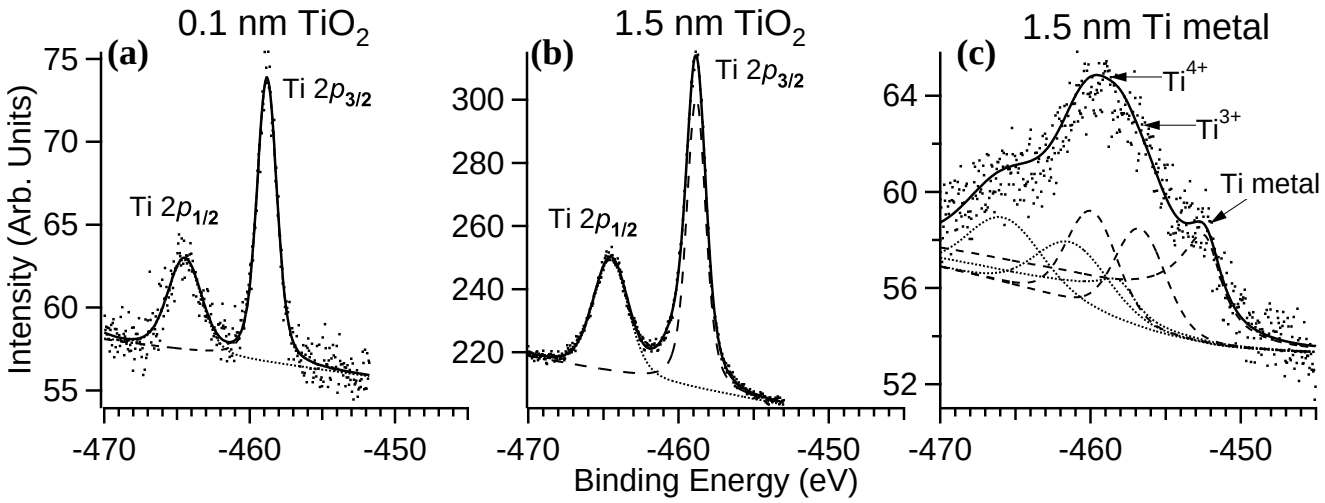

FIG. 3: **Ti 2*p* core-level x-ray photoelectron spectroscopy.** Ti 2*p* XPS spectra of (a) 0.1 nm TiO_2, (b) 1.5 nm TiO_2, and (c) 1.5 nm Ti metal. All XPS spectra were taken *in situ* using Mg K_α radiation. Dots are raw data points, dashed and dotted curves are Ti $2p_{3/2}$ and $2p_{1/2}$ individual peak-fit lines, and solid curves are the summed fits. The additional peaks at 458 eV, 461 eV, and 466 eV (dotted curves) in (c) are the Ti $2p_{1/2}$ spin-orbit peak from the Ti^{0+}, Ti^{3+}, and Ti^{4+} oxidation states, respectively. Growth conditions were identical for (a-c), except for (c), where $P_{O_2} < 1{\times}10^{-10}$ torr. Note the multiple oxidation states of Ti when pure metal is evaporated on LAO(001), (c).

the step edges (region between ∼11 nm and ∼16 nm). The predominance of steps of height d indicates similar monolayer-high islands of TiO_2 on both La-O and Al-O_2 surface terminations. ISS showed partial coverage of both surface terminations, with reduced, but still measurable, scattering from both Al and La, in addition to O and Ti. No large-scale second-layer TiO_2 nucleation is observed before the first layer coalesces.

Continued growth of TiO_2 results in fairly uniform coverage of the substrate, with predominately single-height steps after about 4-5 molecular layers of deposition [Fig. 1(c)]. Again, distinct, ∼150 nm wide terraces separated in height by $2d$ are observed in the larger scale image [Fig. 1(c)]; the edges are more clearly aligned with the [010] direction than for the bare LAO [Fig. 1(a)] or initial growth [Fig. 1(b)]. This may be a result of the lower measurement temperature (room temperature *vs.* 400°C), individual sample differences in miscut angle, or the TiO_2 growth itself.

High resolution STM [Fig. 2(c)] shows that the TiO_2(001) film exhibits ∼8-10 nm diameter domains containing bright rows in groups of 3 or 4 oriented along either [100] or [010]. The observed ∼1.8-2 nm spacing between rows is within our calibration error in this variable-temperature experiment of the 1.6 nm spacing of the well-studied 1×4 reconstruction of anatase (001)[17–20]. A similar morphology containing small domains in both [100] and [010] orientation is seen for anatase films grown on $SrTiO_3$[18,20]. However, we observe an additional modulation of the rows in the perpendicular direction, also with a length scale on the order of 2 nm. Of significant importance in Fig. 2(c) is the uniformity in coverage of the LAO by the TiO_2 film, confirming TiO_2 nucleation on both surface terminations of LAO(001). The height variations along the line connecting points C and C′ [Fig. 2(f)] show multiple step heights; combining the $d_{LAO} = 0.19$ nm step of the substrate, the $d_{TiO_2} = 0.24$ nm layer spacing in the anatase film, plus the additional corrugation of the surface reconstruction.

Figs. 3(a-c) show Ti 2*p* photoemission using Mg K_α radiation. The first two spectra [Figs. 3(a,b)] are for the same 0.1 and 1.5 nm films as in Figs. 1(b,c). The last spectrum [Fig. 3(c)] is from a Ti film with the same Ti exposure as for the film in Fig. 1(c), but deposited in the absence of O_2 ($P_{O_2} < 1{\times}10^{-10}$ torr). The subML and thicker TiO_2 films both show a distinctive Ti^{4+} oxidation peak at 459 eV binding energy (BE) with no significant contributions from intermediate oxidation states. In contrast to these spectra, the Ti metal XPS shows multiple Ti oxidation states, with roughly half the Ti in oxidized Ti^{3+} and Ti^{4+} states, with the other half remaining as metallic Ti^0. The dashed and dotted curves in Figs. 3(a-c) are the individual peak-fit lines for the Ti $2p_{3/2}$ and $2p_{1/2}$ states, respectively. The additional peaks at 458 eV, 461 eV, and 466 eV (dotted curves) in Fig. 3(c) are the Ti $2p_{1/2}$ spin-orbit peak from the Ti^{0+}, Ti^{3+}, and Ti^{4+} oxidation states, respectively.

The crystal phase of TiO_2 films grown under similar conditions to those for which data are presented here was verified to be anatase using the soft x-ray absorption near edge structure (XANES) of the Ti L-edge and O K-edge (data taken at the Advanced Light Source in Berkeley, CA, Beamline 7.0.1). Our XANES results were consistent with previously published data for both bulk anatase[21–24] and thin film TiO_2 on LAO(001)[8,11], and

distinctly different from our measurements on a rutile standard.

IV. DISCUSSION

We first discuss the high-temperature (400°C) termination of LAO(001). Our results indicate a base terrace of a single termination, with about half that surface covered by single-height step islands; these islands would be of the opposite termination in the bulk LAO crystal structure. Surfaces covered by a single, unreconstructed $(\text{La-O})^+$ or $(\text{Al-O}_2)^-$ termination would be electrostatically unstable due to the uncompensated surface dipole. The simplest way to stabilize the surface is for the surface layer to be half-occupied on a scale less than the surface electrostatic screening length. It is unlikely that the observed 10-20 nm scale of the alternating terminations is small enough to fully cancel the dipole, although the insensitivity of nc-AFM to these islands is indicative of a long-range Coulomb interaction of these alternately-charged terminations. Alternative solutions for surface charge balance include reconstruction to reduce the surface charge by half, *e.g.*, 1/4 monolayer of oxygen vacancies (for Al-O_2) or adatoms (for La-O).

A schematic of LAO(001) with multiple step and terrace configurations is shown in Fig. 4. Our combined STM and ISS results do not distinguish between an La-O base with Al-O_2 islands and vice versa. Since the $(\text{La-O})^+$ termination can be neutralized by oxygen adsorption, annealing in O_2 at 670°C would favor La-O termination; subsequent heating to 400°C in UHV for imaging could then etch the La-O, leaving La-O islands on an Al-O_2 base. On the other hand, if the surface starts out as Al-O_2 terminated, which has been reported at room temperature[12–15], then O_2 annealing might etch the Al-O_2 surface layer to form single-height Al-O_2 islands on a La-O base. The similarity in island structure before and after TiO_2 deposition (compare panels (a) and (b) in Figs. 1and Figs. 2) reflects the approximate morphology and surface termination during TiO_2 growth, which occurred under oxygen rich conditions at 570°C.

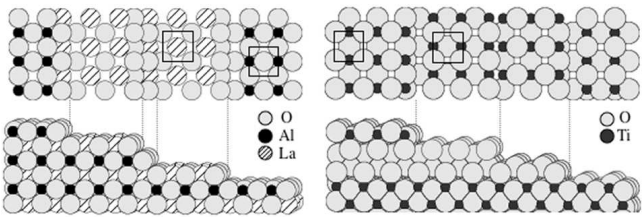

FIG. 4: **Schematic of LAO(001) surface termination.** Left: LAO(001); Right; Anatase (001). Bottom: 3-D view along [010] direction, with the spheres having the appropriate ionic radii. Top: Planar view of the stepped (001) surface. Lower levels included only at step edges. Boxes denote 1×1 surface unit cells. Steps are shown in oxygen-rich configuration.

The observed TiO_2 nucleation at step edges, independent of the cation termination of the upper or lower terrace, implies Ti prefers attaching to under-coordinated surface oxygen species at the steps (see Fig. 4), independent of the cation or number of oxygen atoms in the adjacent terrace. The question then arises as to why we observe subsequent growth of TiO_2 across both La-O and Al-O_2 terraces with roughly equal probability.

The anatase layer structure is close to that of the Al-O_2 layer, with a small buckling to adjust the bond length; we thus expect straight-forward epitaxy on the La-O termination. In bulk LAO, La-O layers donate a formal charge of 0.5 electrons to each adjacent Al-O_2 layer; donating this charge to a TiO_2 layer would result in a mixed valence $Ti^{3+/4+}$ structure with a conducting interface.[6] Although we do not observe a significant Ti^{3+} contribution in XPS at the interface, we do observe sufficient conduction in our films for conductive tunneling at room temperature once the film has coalesced, indicating a possible mixed valence interface. It is also possible that substitution of La^{3+} or Al^{3+} in the TiO_2 layer could lead to electronic conductivity without Ti^{3+}.

The low energy sites above an Al-O_2 termination accommodate only a single positive and negative ion, with a separation $\sim 40\%$ larger than the Al-O (or Ti-O) spacing. One possible growth mode is substitution of Ti for surface Al, perhaps with compensating oxygen vacancies in the interface layers. The extensive partial oxidation of Ti metal in the absence of an O_2 flux [Fig. 3(c)] indicates some substrate cation−oxygen bonds may be replaced by Ti-O bonding. Substitution of Ti for Al would place the first TiO_2 layer in a more favorable site than would direct adsorption on Al-O_2; replacement of half the Al^{3+} by Ti^{4+} would also compensate for the formal 0.5 electron normally supplied by the adjacent La-O layer.

After the TiO_2 films coalesce, memory of the initial nucleation is reflected in the domain structure of the anatase surface reconstruction. The average domain size in Fig. 2(c) is comparable to both the island width and the spacing between TiO_2 nuclei in Fig. 2(b). In bulk anatase, (001) layers alternate between Ti-O bonds parallel to [100] and to [010] (see Fig. 4), so that the 1×4 reconstruction rotates by 90° and translates between adjacent terraces. The symmetry of both the La-O and Al-O_2 surface terminations of LAO(001) is such that [100] and [010] orientations of TiO_2 molecules would nucleate with equal probability.

The pattern of TiO_2 domains observed in Fig. 2(c) likely has three causes: 1) TiO_2 domains nucleated at 90° to each other on the same substrate terrace; 2) TiO_2 domains nucleating independently, parallel to each other, on adjacent substrate terraces; and 3) single-crystal TiO_2 domains containing a surface step that rotates the domain by 90°. These would result in adjacent rotated domains having the same height, heights differing by d_{LAO}, or heights differing by d_{TiO_2}, respectively. Our data are consistent with all three processes occurring, though it is not possible to decouple the last two within our experi-

mental resolution.

V. SUMMARY

In summary, we have shown that annealing $LaAlO_3(001)$ substrates in 5×10^{-5} torr of molecular O_2 and subsequently heating to 400°C in UHV produces a surface consisting of one base termination (either La-O or Al-O_2) with about half the surface covered by single-layer high islands of the alternate surface termination. Alternating surface terminations has minimal effect on nucleation and growth of the single metal oxide TiO_2. Epitaxial anatase uniformly covers both terminations, in ∼10 nm domains with two orthogonal surface layer orientation. The TiO_2 nucleates near steps, likely at undercoordinated oxygen sites.

Acknowledgments

This work is supported by NSF Grant ECS 0224138 and M. J. Murdock Charitable Trust. D. A. S. further acknowledges support from UW-PNNL Joint Institute for Nanoscience research award and T. O. from the Center for Nanotechnology University Initiative Fund of the University of Washington. The authors acknowledge S. A. Chambers for fruitful discussions and sample standards. The authors further acknowledge F. S. Ohuchi for insightful suggestions.

---

* Present address: International Center for Young Scientists, NIMS, Tsukuba, Japan.
† Present address: Advanced Light Source, Berkeley, CA 94720
‡ Present address: CNT, UW, Seattle, WA 98195-2140

[1] R. W. Simon, C. E. Platt, A. E. Lee, G. S. Lee, K. P. Daly, M. S. Wire, and J. A. Luine, Appl. Phys. Lett. **57**, 1351 (1990).
[2] R. Brown, V. Pendrick, D. Kalokitis, and B. H. T. Chai, Appl. Phys. Lett. **57**, 1351 (1990).
[3] M. V. Jacob, J. Mazierska, N. Savvides, S. Ohshima, and S. Oikawa, Physica C **372-376**, 474 (2002).
[4] T. Stelzner, H. Schneidewind, and G. Bruchlos, IEEE Trans. Appl. Supercon. **13**, 2766 (2003).
[5] D.-W. Kim, D.-H. Kim, B.-S. Kang, T. W. Noh, D. R. Lee, and K.-B. Lee, Appl. Phys. Lett. **74**, 2176 (1999).
[6] A. Ohtomo, and H. Y. Hwang, Nature **427**, 423 (2004).
[7] Y. Matsumoto, M. Murakami, T. Shono, T. Hasegawa, T. Fukumura, M. Kawasaki, P. Ahmet, T. Chikyow, S. Koshihara, and H. Koinuma, Science **291**, 854 (2001).
[8] S. A. Chambers, T. Droubay, C. M. Wang, A. S. Lee, R. F. C. Farrow, L. Folks, V. Deline, and S. Anders, Appl. Phys. Lett. **82**, 1257 (2003).
[9] J.-Y. Kim, J.-H. Park, B.-G. Park, H.-J. Noh, S.-J. Oh, J. S. Yang, D.-H. Kim, S. D. Bu, T.-W. Noh, H.-J. Lin, H.-H. Hsieh, and C. T. Chen, Phys. Rev. Lett. **90**, 017401 (2003).
[10] S. R. Shinde, S. B. Ogale, S. Das Sharma, J. R. Simpson, H. D. Drew, S. E. Lofland, C. Lanci, J. P. Buban, and N. D. Browning, Phys. Rev. B. **67**, 115211 (2003).
[11] M. Murakami, Y. Matsumoto, K. Nakajima, T. Makino, Y. Segawa, T. Chikyow, P. Ahmet, M. Kawasaki, and H. Koinuma, Phys. Rev. Lett. **78**, 2664 (2001).
[12] J.-P. Jacobs, M. A. S. Miguel, and L. J. Álvarez, J. Mol. Struct. **390**, 193 (1997).
[13] J.-P. Jacobs, M. A. S. Miguel, J. E. Sánchez-Sánchez, and L. J. Álvarez, Surf. Sci. **389**, L1147 (1997).
[14] P. A. W. van der Heide and J. W. Rabalais, Chem. Phys. Lett. **297**, 350 (1998).
[15] J. Yao, P. B. Miguel, S. S. Perry, D. Marton, and J. W. Rabalais, J. Chem. Phys. **108**, 1645 (1998).
[16] H. Kawanowa, H. Ozawa, M. Ohtsuki, Y. Gotoh, and R. Souda, Surf. Sci. **506**, 87 (2002).
[17] G. S. Herman, M. R. Sievers, and Y. Gao, Phys. Rev. Lett. **84**, 3354 (2000).
[18] Y. Liang, S. Gan, S. Chambers, and E. Altman, Phys. Rev. B **63**, 235402 (2001).
[19] M. Lazzeri, and A. Selloni, Phys. Rev. Lett. **87**, 266105 (2001).
[20] R. E. Tanner, Y. Liang, and E. Altman, Surf. Sci. **506**, 251 (2002).
[21] F. M. F. de Groot, J. C. Fuggle, B. T. Thole, and G. A. Sawatzky, Phys. Rev. B **41**, 928 (1990).
[22] J. P. Crocombette and F. Jollet, J. Phys.: Condens. Matter **6**, 10811 (1994).
[23] G. van der Laan, Phys. Rev. B **41**, 12366 (1990).
[24] R. Ruus, A. Kikas, A. Ausmees, E. Nõmmiste, J. Aarik, A. Aidla, T. Uustare, and I. Martinson, Solid State Comm. **104**, 199 (1997).